An Unexpected Tetragonal Network of Seven-Connected Er_6 Clusters Stabilized by Multiple Halogen Bonds through Cooperative Effects

Jonas Braun,* Christian Pachl, Olaf Fuhr, George E. Kostakis, Jinkui Tang, Christopher E. Anson, Karin Fink,* and Annie K. Powell*

ABSTRACT: Halogen bonding is increasingly recognized as a further elaboration of supramolecular effects b etween c oordination m oieties. Here, we report two isostructural trigonal prismatic Er_6 coordination clusters for which one has no halogen on the ligand (*E*)-*N*′-(2-hydroxy-3-ethox ybenzylidene)pyrazine-2-carbohydrazide (H_2oepch) (**1**), whereas the other has a bromine on the *o*-vanillin component (*E*)-*N*′-(5-bromo-2-hydroxy-3-methoxybenzylidene)pyrazine-2-carbohydrazide (H_2opch-Br) (**2**). This allows us to gauge the effect of the supramolecular interactions on network formation via halogen bonding. Furthermore, the topological analysis on the network in (**2**) reveals a completely novel and unexpectedly 7-connected uninodal network that has to conform with the symmetry imposed by the tetragonal space group $P\bar{4}2_1c$. In addition, in-depth theoretical calculations were performed to investigate the strength of the halogen bonding interactions and reveal cooperative effects unprecedented for inorganic coordination clusters.

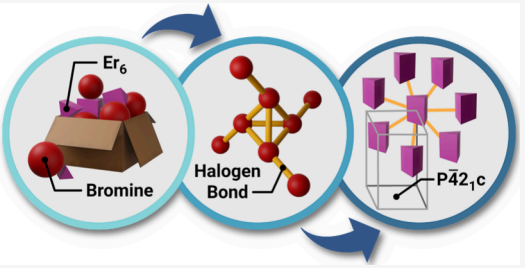

INTRODUCTION

Intermolecular interactions are used in supramolecular chemistry to produce compounds with a wide range of properties.[1−4] Furthermore, they are a powerful tool which can be used to steer the crystallization of compounds and thereby design supramolecular architectures which may amplify the desired properties.[5−9] Among these interactions the most familiar ones are hydrogen bonds (HBs),[10,11] π-interactions[12−17] and van der Waals forces[18−21] which can be found in a plethora of both naturally occurring and synthetic organic and inorganic compounds.[22−25]

In addition to the interactions mentioned above, halogen interactions have been studied since the 1950s when pioneering work by Hassel revealed attractive intermolecular interactions between solvents and Br_2 in which the electronegative halogen atoms act as electron density acceptors.[26−28] Although this initially seems counterintuitive since the distribution of the electron pairs around an isolated halogen atom is spherical, theoretical studies show that in halogens which are covalently linked to other atoms this is no longer the case. Instead, it was found that the electron density of the halogen atom is arranged in a belt orthogonal to the covalent bond. This results in an area of low electron density on the opposite side of this covalent bond.[29] This electropositive area known as the sigma hole can interact attractively with electron density donors such as π-systems, lone pairs on other atoms such as nitrogen or other halogen atoms. These halogen interactions are abbreviated as XB in analogy to HBs. The electron density donor in an XB is defined as the XB acceptor (XB_A) and the halogen providing the sigma hole is defined as XB donor (XB_D).[26,30−32] When the XB_A is a second halogen atom, this results in two types of halogen−halogen interactions. The idealized geometry for such interactions in an $R{-}X_D{\cdots}X_A{-}R'$ system are angles of 180° and 90° at X_D and X_A, respectively.

As a result of the high degree of directionality they provide by the lone pair-sigma hole interactions, halogen bonds can be harnessed to aid in molecular structure engineering.[33−35] Whereas this is often used in the crystal design of organic compounds,[26] it is rare in magnetic coordination clusters.[36−40] However, there are examples where it was shown that halogen bonding provides a pathway for spin transitions and can alter magnetic interactions.[41−43]

The nature of halogen bonding has a long history. Originally, the mechanism was described as a charge-transfer[27,44] or else an electron donor−acceptor interaction.[45−47] This perception changed in the 1990s when Politzer and Murray described halogen bonding as an electrostatic interaction.[31,48] Nowadays, more convoluted energy decomposition schemes have been

Scheme 1. Structures of the Schiff Base Ligands H_2oepch and H_2opch-Br That Were Used to Produce Compounds 1 and 2, Respectively

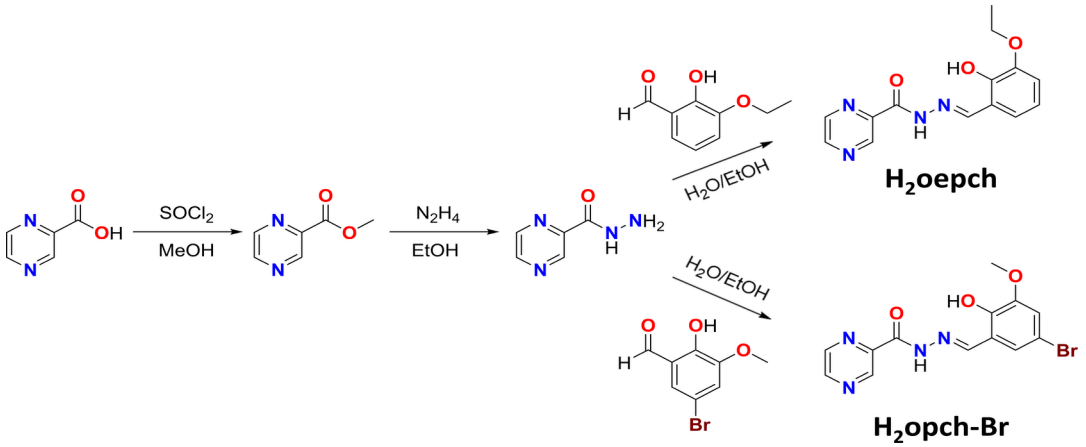

used to explain the bonding, recognizing the simultaneous interaction through orbital interaction, lone pair repulsion and electrostatic interactions.[49,50] The importance of London dispersion to describe the total interaction energy is generally accepted.[51,52] Current research revolves around the question as to whether the σ-hole is an intrinsic property of the XB_D or if it can be induced by the bonding partner.[33] Whether or not to include the basis set superposition error in calculations[53,54] and the question of possible covalency in halogen bonds have recently been revisited.[55]

Analogous to the situation in hydrogen bonds, cumulative additional stabilization can be achieved when a molecule or atom is involved in multiple bonds. The bonding energy is thus more than the sum of its parts.

$$E_{total} = \sum_{pairs} E_{pair} + E_{syn}$$

This nonadditive contribution is a synergy/cooperative effect for a given cluster and is well established for water cluster structures.[56,57] Recent studies have shown such effects for multiple halogen bonds interacting with each other. Investigations into XB-triangles,[58,59] squares[60] and larger molecular assemblies (clusters)[61−63] have shown strong synergy effects for the idealized geometrical arrangements. Calculations on infinite chains indicate that synergy effects will increase with the number of interacting monomers up to a given limit.[64,65] Additionally, there is theoretical evidence for negative cooperativity in particular situations, where a halogen bond is destabilized by addition of another nearby XB.[66] Whereas all the aforementioned examples discuss theoretical model systems, one of the rare examples in which calculations were carried out on a real system involved halogen bonds in cyclic *N*-halo-guanine quartets.[67] The present study is the first demonstration of cooperativity in a network based on coordination clusters.

Here, we explore the influence of halogen bonding on the crystal packing of lanthanide complexes. The chosen system can be modified by using a Schiff base ligand to which a Br substituent can be added to support the formation of halogen bonds while maintaining the metal cluster core structure. The results here represent the first example of a physical coordination compound as opposed to a model system where cooperative effects are substantiated from a theoretical standpoint.

GOAL AND REALIZATION

The main objective of the present study was to explore the use of halogen substituents on the ligand in order to induce supramolecular halogen interactions and influence the crystal packing. A strongly connected network of coordination clusters could indeed be obtained, as established from single crystal X-ray crystallography. Crystals of Er^{III}_6 clusters suitable for crystallographic analysis were obtained and the respective structures are described below. In addition, we were able to investigate the influence of the strength of halogen interactions on the packing. The effects of the halogen bonding were compared to the changes of the steric hindrance of the ligand alkoxy group. In addition, magnetic data were recorded on the complexes although this was not the main focus of this study. Given the lack of slow magnetic relaxation in compounds **1** and **2**, the potential influence of halogen bonding networks on magnetic relaxation mechanisms will be part of further investigations using other perhaps more magnetically interesting ions such as Dy^{III} (see Section 2 in the SI for further details on the magnetic data).

RESULTS AND DISCUSSION

Here we report two Er^{III}_6 coordination clusters based on the same CO_3^{2-}-bridged trigonal prismatic structural motif using H_2opch type ligands (see Scheme 1).[42,68−72] The first cluster $[Er_6(Cl)_2(CO_3)_2(H_2O)(MeOH)_3(oepch)_6]\cdot 2H_2O\cdot 9MeOH$ (**1**) was synthesized using (*E*)-*N*′-(2-hydroxy-3-ethoxybenzylidene)pyrazine-2-carbohydrazide (H_2oepch) while the second compound $[Er_6(Cl)_2(CO_3)_2(H_2O)_3(MeOH)(opch\text{-}Br)_6]\cdot 2MeOH$ (**2**) has (*E*)-*N*′-(5-bromo-2-hydroxy-3-methoxybenzylidene)-pyrazine-2-carbohydrazide (H_2opch-Br) as the main ligand. Both clusters are held together by two μ_3-bridging carbonate ligands that are derived from aerial CO_2 fixation which is increasingly recognized as a feature of lanthanide containing coordination compounds.[72−75] This is not surprising given the role of lanthanide carbonate minerals in the Earth's crust.[76]

CRYSTALLOGRAPHY

In order to compare the effect of steric hindrance vs halogen bonding on the packing and molecular structure of these Ln_6 complexes, in addition to compounds **1** and **2**, two further compounds have been considered. The four compounds are

coordinated by the following four ligands, respectively (see Scheme 2).

Scheme 2. Structures of the Four H_2opch-Type Ligands Used for the Compounds Described Here[a]

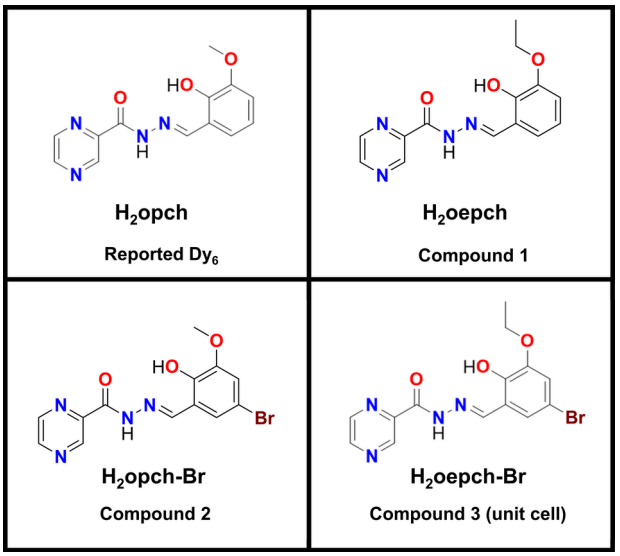

[a]The original H_2opch ligand was used by Tang et al. to produce the published Dy_6 cluster (top left).[68] This work has implemented an ethoxy group (H_2oepch, top right), a bromine atom (H_2opch-Br, bottom left) and a version of the ligand with both, the ethoxy group and the Br atom (H_2oepch-Br bottom right). The crystal structures of the Er_6 clusters resulting from the usage of H_2oepch (compound **1**) and H_2opch-Br (compound **2**) are analyzed in the following to gauge the effect of the ligand modifications on the crystal packing. Of compound **3** using H_2oepch-Br only a unit cell could be determined as further outlined below.

Compound **1** crystallizes in the triclinic space group $P\bar{1}$ with Z = 2. The molecular structure is very similar to that of the previously reported Dy_6 compound[68] (see Figure S1) and the structure will therefore be only briefly described here. Pairs of Er^{3+} ions are bridged by the carboxyhydrazide oxygens of the doubly deprotonated $(oepch)^{2-}$ ligands. These are arranged in a head-to-tail fashion, such that each Er^{III} is further ligated by a carboxyhydrazide N atom and phenoxido O atom from one ligand, and by a pyrazine N atom from the other ligand. Three such Er_2 dimeric units are then linked by two symmetrically bridging carbonates, forming the two $Er_3(\mu_3,\eta^3\text{-}CO_3)$ triangular faces of the trigonal-prismatic Er_6 core. The coordination environments of the Er^{III} ions are completed by terminal ligands, two chlorides, three methanols and one water; the cluster molecule is thus neutral. Compound **2** crystallizes in the tetragonal space group $P\bar{4}2_1c$ with $Z = 8$. Apart from the obvious presence of the bromo-substituents on the $(Br\text{-}opch)^{2-}$ ligands, the only slight differences between the molecular structures of **2** (Figures 1 and S1, S2) and **1** are the replacement of the ethoxy groups on the ligands in **1** with methoxys in **2**, and that one of the chlorides in **2** is disordered against aqua ligands over three Er centers.

The clusters in **1** are linked over inversion centers via pairs of hydrogen bonds between water ligands and pyrazine N atoms and $\pi-\pi$ interactions into supramolecular dimers (Figure S3). The previously reported $Dy_6(opch)_6$ cluster was found to be linked into 1-D chains in the crystal, although the linkages here

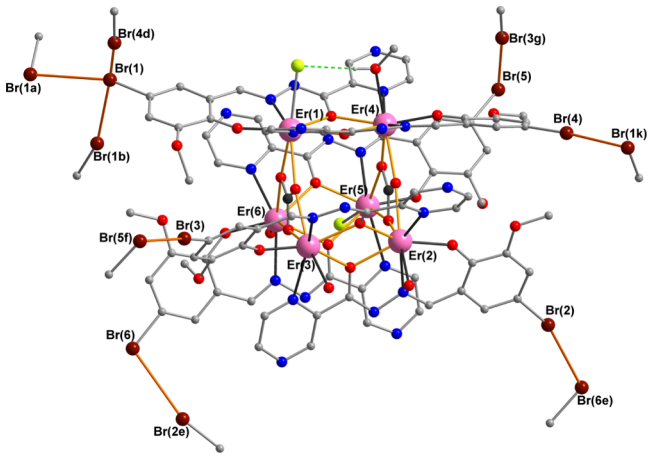

Figure 1. Molecular structure of the Er_6 cluster in **2**, showing the eight halogen bonds. Er pink, Br brown, O red, N blue, C gray, Cl pale green, Er−O(bridging) yellow, Br···Br orange. Symmetry codes: a: $y, -x, 1-z$. b: $-y, x, 1-z$. d: $\frac{1}{2}-x, -\frac{1}{2}+y, \frac{1}{2}-z$. e: $-x, 1-y, z$. f: $-\frac{1}{2}+x, \frac{1}{2}-y, \frac{1}{2}-z$. g: $\frac{1}{2}+x, \frac{1}{2}-y, \frac{1}{2}-z$. k: $\frac{1}{2}-x, \frac{1}{2}+y, \frac{1}{2}-z$.

were weaker, involving rather long C−H···N hydrogen bonds.[68] By contrast, the clusters in **2** are linked into a 3-D network by multiple halogen bonds involving the ligand bromine atoms (see Figure 2). Here the effect of the bromine atom on the ligand outweighs the slight difference in steric hindrance by replacing ethoxy with methoxy. This can be shown by looking at the isostructural Er_6 compound (**3**) using the ligand with both the ethoxy group and the bromine atom (H_2oepch-Br, see Scheme 2 above). This compound crystallizes isomorphously to compound **2** in $P\bar{4}2_1c$ (with $a = 30.0980(6)$ Å and $c = 26.7876(6)$ Å) and thus forms the same halogen bonded network, although the very small size of the crystals precluded a full refinement of the structure. This indicates that the stabilization through the halogen-bonded network has a much larger influence on the packing than the respective steric bulks of the methoxy and ethoxy groups.

Five of the six Br atoms in a molecule in **2** are involved in such interactions, while Br1 is involved in three halogen bonds. These halogen bonds all have Br−Br distances less than the sum of two van der Waals radii for Br (3.75 Å),[77] and their geometries are listed in Table 1. All of these interactions have one C−Br···Br angle close to 180° and the other close to 90°.[26]

Three distinct halogen bond motifs in **2** link the cluster molecules (Figure 2).

The first of these involves eight distinct clusters (Figure 2a). Four Br1 atoms related by crystallographic $\bar{4}$ site symmetry form a compressed tetrahedron. Four edges of this tetrahedron correspond to halogen bonds and have Br−Br distances of 3.573(2) Å while the other two edges are longer (3.939(3) Å), longer than twice the VdW radius of Br and are shown as dashed lines in Figure 2a,b). Each of these four bromines is involved in a further halogen bond to a symmetry-equivalent of Br4. For clarity, these eight bromines, together with the aromatic rings to which they are bonded, are shown in Figure 2b with the same viewing directions as in Figure 2a.

In order to visualize the symmetry of this central motif which dictates the symmetry of the crystals structure, Scheme 3 shows how the arrangement of the four Br1 atoms varies from tetrahedral. The tetrahedron (T_d) is compressed leading to D_{2d}

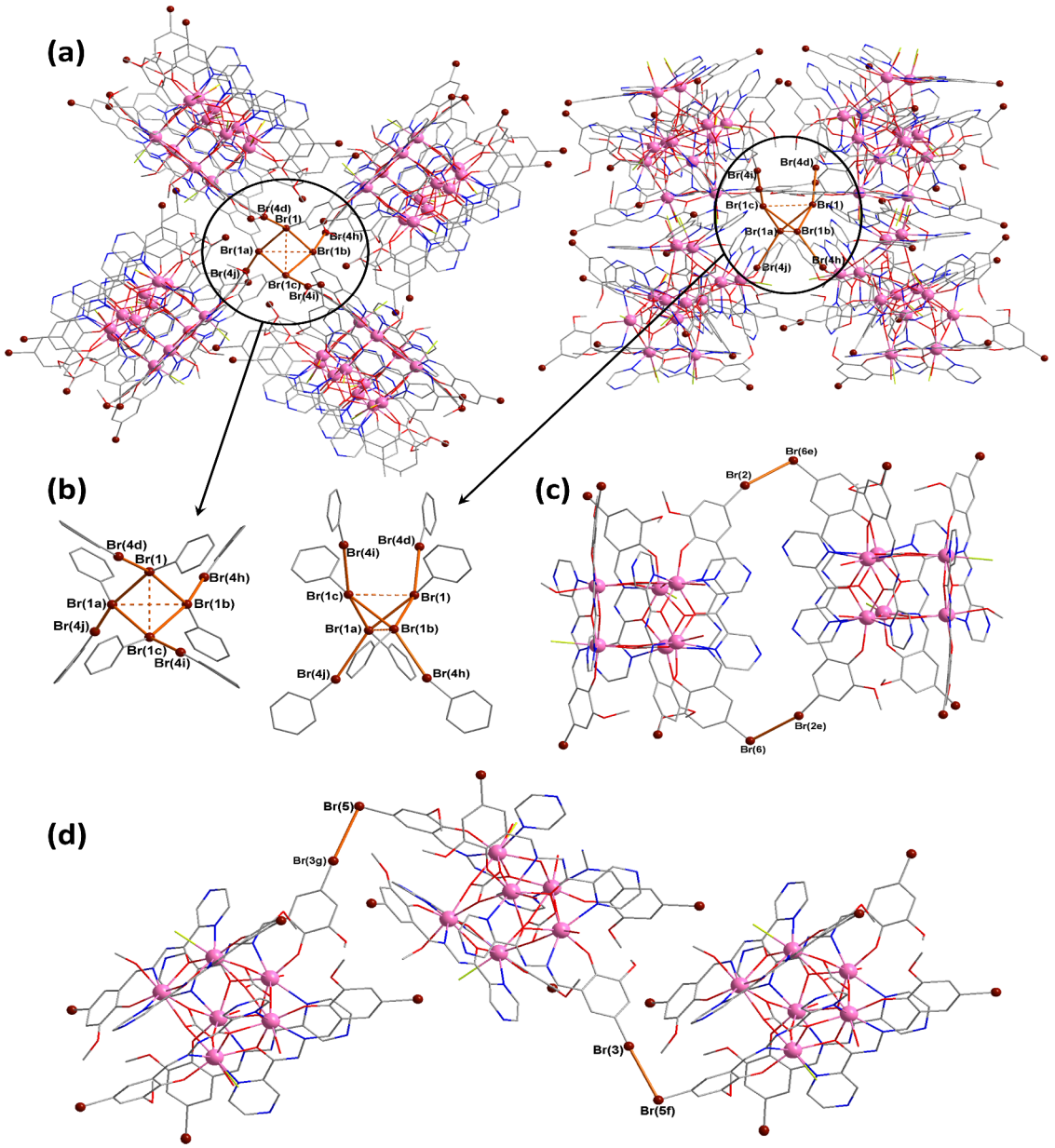

Figure 2. Br···Br interactions observed in the crystal structure of **2**: (a) interactions involving Br1 and Br4 (and their symmetry equivalents) centers about a $\bar{4}$ site and linking eight clusters, viewed along the *c* and *a* axes. (b) as (a), but for clarity showing only the Br atoms and the aromatic rings to which they are bonded. (c) Interactions involving Br2 and Br6 between two molecules related by a C_2-rotation axis. (d) Interactions involving Br3 and Br5 between molecules related by a 2_1 screw axis. Br−Br halogen bonds shown as orange lines. The dashed orange lines in (a) and (b) do not correspond to bonds, but guide the eye in visualizing the compressed tetrahedron of four Br atoms at the center of the $\bar{4}$ assembly. Symmetry codes: a: $y, -x, 1-z$. b: $-y, x, 1-z$. c: $-x, -y, z$. d: $\frac{1}{2}-x, -\frac{1}{2}+y, \frac{1}{2}-z$. e: $-x, 1-y, z$. f: $-\frac{1}{2}+x, \frac{1}{2}-y, \frac{1}{2}-z$. g: $\frac{1}{2}+x, \frac{1}{2}-y, \frac{1}{2}-z$. h: $\frac{1}{2}-y, \frac{1}{2}-x, \frac{1}{2}+z$. i: $-\frac{1}{2}+x, \frac{1}{2}-y, \frac{1}{2}-z$, j: $-\frac{1}{2}+y, -\frac{1}{2}+x, \frac{1}{2}+z$.

symmetry and the two elongated Br1−Br1 contacts now highlighted in orange. The involvement of the four halogen-bonded Br4 atoms then leads to the observed S_4 symmetry.

The second motif, involving Br2 and Br6, provides pairwise linkages between molecules which are related by a C_2 axis (Figure 2c).

Finally, single halogen bonds involving Br3 and Br5 link clusters related by the 2_1 screw axes into chains parallel to the crystal *a*- or *b*-axis (Figure 2d).

Since each individual Er_6 cluster is involved in eight halogen bonds, two of which (those involving Br2 and Br6) are to the same neighboring molecule, a single Er_6 cluster is therefore directly linked by halogen bonding to seven other clusters. This is shown in Figure 3, where the centroid of the central cluster is shown as connected to the surrounding clusters by orange dashed lines, while the centroids of the seven surrounding clusters are joined by black dashed lines, showing the polyhedron, they form.

TOPOLOGICAL ANALYSIS

The combination of these three motifs links the Er_6 clusters in **2** into a tetragonal 3-D network. This is shown schematically in Figure 4, where the clusters are shown as trigonal prisms and the

Table 1. Geometries for the C−Br···Br−C Interactions in the Crystal Structure of 2

interaction	C−Br···Br (°)	Br···Br (Å)	Br···Br−C (°)	symmetry code
C45−Br1··· Br1[a]−C45[a]	162.9(4)	3.573(2)	98.5(3)	a: $y, -x, 1-z$
C45−Br1··· Br1[b]−C45[b]	98.5(3)	3.573(2)	162.9(4)	b: $-y, x, 1-z$
C45−Br1··· Br1[c]−C45[c]	108.5(5)	3.939(3)[a]	108.5(5)	c: $-x, -y, z$
C45−Br1··· Br4[d]−C32[d]	74.5(4)	3.643(2)	163.5(6)	d: $^1/_2 - x, -^1/_2 + y, ^1/_2 - z$
C6−Br2···Br6[e]−C71[e]	162.0(4)	3.580(2)	108.2(3)	e: $-x, 1-y, z$
C19−Br3··· Br5[f]−C58[f]	175.6(4)	3.680(2)	92.5(3)	f: $-^1/_2 + x, ^1/_2 - y, ^1/_2 - z$
Br5−C58··· C19[g]−Br3[g]	92.5(3)	3.680(2)	175.6(4)	g: $^1/_2 + x, ^1/_2 - y, ^1/_2 - z$

[a]Distance longer than twice the VdW radius of Br (1.85 Å) and thus not considered a halogen−halogen bond. However, perhaps unexpectedly, it is shown in the calculations presented below that this short contact adds to the stabilization of the central motif and the overall crystal packing (see Table 2).

Scheme 3. Topology of the Central Halogen Bond Arrangement (in the Following Also Halogen Bond Cluster, XB-Cluster) within 2[a]

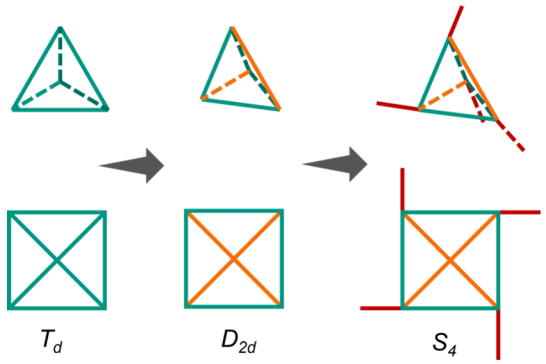

[a]The top row displays a side view of the cluster, whereas the bottom row is the view along the *c*-axis (the same viewing direction as Figure 2a). Each vertex represents a bromine atom, while each line represents a halogen bond. Starting from a regular tetrahedron (T_d) (as it appears looking down the crystallographic *c* axis), two opposite edges are moved towards each other, reducing the symmetry to D_{2d}. Subsequently, each edge is elongated to form another halogen bond leading to the S_4 symmetry observed in **2**.

halogen bonds are represented by straight lines joining the vertices of each Er_6 trigonal prism. These lines are color-coded for clarity, with the bonds in the Br1/Br4 $\bar{4}$ motifs in orange, those between Br2 and Br6 in green, and between Br3 and Br5 in cyan. From the zero value for the Flack parameter, $\chi = -0.023(2)$, from the final refinement of the structure of **2**, it is clear that the handedness of the chiral network is maintained throughout the crystal, so that a given crystal is enantiomerically pure.

The topological classification of metal−organic frameworks (MOFs) and their analysis as networks have greatly facilitated the understanding of MOF synthesis and representation, making the field more accessible and widely recognized. This classification translates three-dimensional networks, typically constructed from covalent bonds, into simplified topological

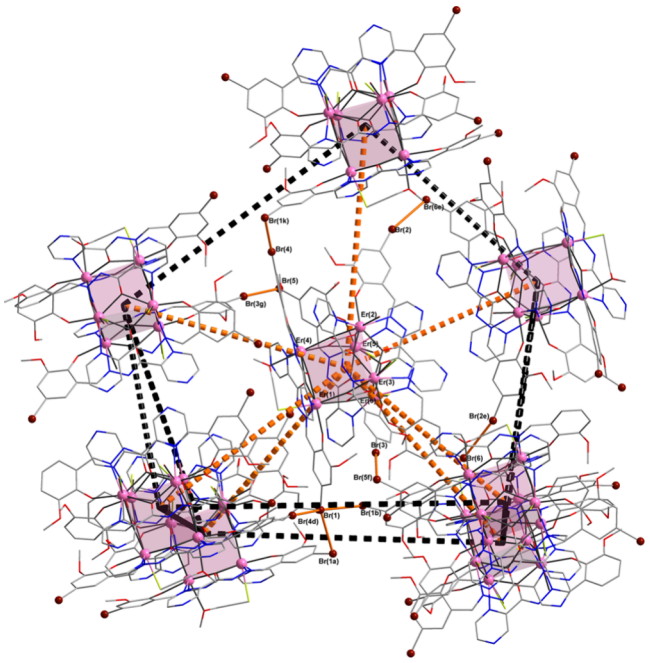

Figure 3. Linkage of an Er_6 cluster to seven surrounding clusters by halogen bonding. The centroid of the trigonal prismatic core of the central Er_6 is joined to the centroids of the surrounding clusters by orange dashed lines, while the centroids of the surrounding clusters are themselves joined by black dashed lines.

models. Covalent bonds, due to their strong electron-sharing nature, are significantly more stable than halogen−halogen bonds.

The topology of the network constructed through the Br−Br interactions in compound **2** was evaluated since it is shown below that the cooperative effects of the halogen bonding constitute a significant stabilization effect of the crystal packing. This analysis revealed an unusual and unique motif: a seven-connected uninodal network within a crystal structure of tetragonal symmetry. The network has the point symbol $\{3^3.4^8.5^8.6^2\}$ and extended point symbol [3.3.3.4.4.4.4.4.4.4 (3).4(3).5.5.5(2).5(2).5(3).5(3).5(3).5(4).6(4).6(7)].[78]

QUANTUM CHEMICAL CALCULATIONS OF BR−BR PAIR INTERACTIONS IN 2

Methodology. In order to assess the intermolecular interactions induced by the halogen bonds, 5-bromo-*ortho*-vanillin was used as a model system. Here the *o*-vanillin unit of the $(opch\text{-}Br)^{2-}$ ligands participating in the interaction were selected from the overall structure. The imine N of the $(opch\text{-}Br)^{2-}$ ligand was replaced by O and the coordinated Er^{III} ions by a proton to preserve charge neutrality. This results in 5-bromo-*o*-vanillin molecules. One should note at this point that it was previously shown that the energy and cooperative effects of XBs depend on the substitution of the phenyl-rings.[50,79] Therefore, two alternative models are discussed in the SI, Table S2. To mimic the interaction in the crystal, the atomic positions were kept as obtained in the refined crystal structure. Only the aldehyde oxygen replacing the imine groups and the hydrogen atoms were optimized.

To gauge the effects of the halogen interaction in terms of the total interaction energy, two calculations were performed. First the interaction was calculated using the model system described above. In a second step the halogen bond was removed by

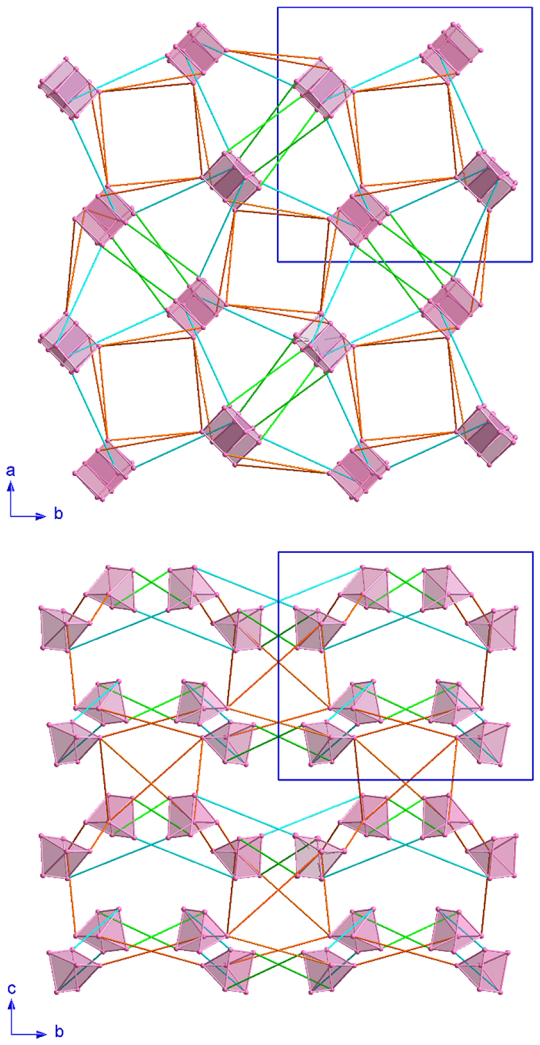

Figure 4. Halogen-bonded network of Er_6 clusters in **2** viewed along the *c*-axis (left) and *a*-axis (right). Clusters shown as pink trigonal prisms and halogen bonds as colored lines (Br1−Br1′ and Br1−Br4′ orange; Br3−Br5′ cyan; Br2−Br6′ green.

replacing the Br-atoms with H atoms which were then optimized. The resulting interaction energy $E_{int,H}$ was subsequently subtracted from the interactions obtained from the calculations involving the XBs $E_{int,X}$ to give the corrected $E_{int,corr}$. The effect of this correction is very small (<1 kJ/mol) in most cases as summarized in Table S3.

$$E_{int,corr} = E_{int,X} - E_{int,H}$$

All calculations were carried out at the DFT/d4[80,81] level using the benchmarked hybrid functionals M06-2X and PBE0 as well as the range-separated CAM-B3LYP.[52,82,83] For further details, see Supporting Information Section 3.

Br−Br Pair Interactions. In total there are five Br−Br pair interactions and the interaction energies obtained using the different functionals are summarized in Table 2. All functionals give similar results within the error limits of general DFT. It can be noted that the M06-2X functional gives a slightly lower energy than the other two, but for a given functional all interactions are similar in magnitude.

Given the longer distance (3.939(3) Å and thus longer than twice the VdW radius of Br) in the diagonal Br1−Br1* contact compared to all other investigated contacts, a significantly lower

Table 2. Interaction Energies and Properties at the Bond Critical Points for Calculated for Pair Interactions Observed in Compound 2[a]

interaction	M06-2X	PBE0	CAM-B3LYP	average	ρ	$\nabla^2\rho$
Br1−Br1	−4.0	−6.1	−5.6	−5.2	0.00920	0.0274
Br1−Br1*	−2.5	−4.6	−4.2	−3.8	0.00541	0.0176
Br1−Br4	−5.8	−7.2	−7.0	−6.7	0.00801	0.0246
Br2−Br6	−4.4	−6.0	−5.6	−5.3	0.00807	0.0246
Br3−Br5	−5.8	−7.8	−7.6	−7.0	0.00656	0.0203

[a]All energies are given in kJ/mol. Characteristics of the BCP are given in atomic units and for the M06-2X functional.

or even zero interaction energy would be expected. However, this is not what we observe from the calculated interaction energies, showing that even interactions not classified as halogen bonds contribute to the stability of the network.

To investigate this further, Bond Critical Points (BCP) were calculated for all the different pair interactions. The BCPs are on the direct Br−Br connection for all interactions. The density ρ at the BCP is lower for interaction Br1−Br1* than for the others, as expected given the long distance between the Br-atoms. However, the Laplacian $\nabla^2\rho$ at the BCP is positive for all interactions including the one between Br1−Br1*. Thus, it can be concluded that there is a bonding interaction present in all cases. A full summary of the BCPs for the different functionals is given in Table S4.

Energy Decomposition Analyses (EDA) were performed. These divide the total interaction energy into different contributions. Here, EDA reveals that dispersion is an essential component in the interactions, since without this the interactions would hardly be attractive in nature. This confirms the importance of dispersion in halogen bonds as previously discussed.[52,84]

All contributions to the total energies of the five investigated interactions are shown in Figure 5, with the values listed in Table S3. Notably, the exchange repulsion is strongly positive for all interactions albeit significantly lower for Br1−Br1* and Br3−Br5 than for the other interactions. For Br1−Br1* this can be easily rationalized given that the exchange repulsion decreases

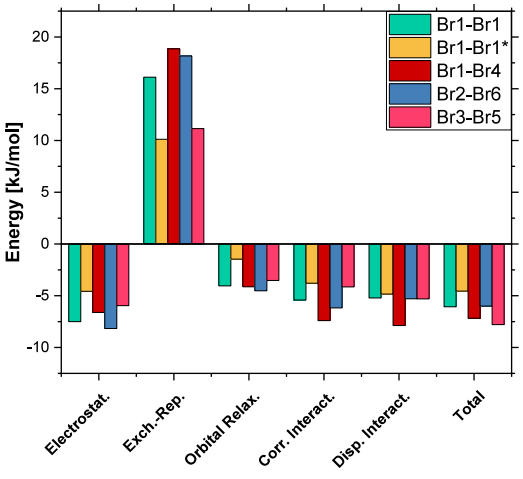

Figure 5. Energy decomposition analysis (EDA) calculated with the functional PBE0 for all 5 pair interactions observed in compound **2**. Electrostatic, Exchange-Repulsion, Orbital Relaxation, Correlation Interaction and the sum of all contributions (Total) are plotted.

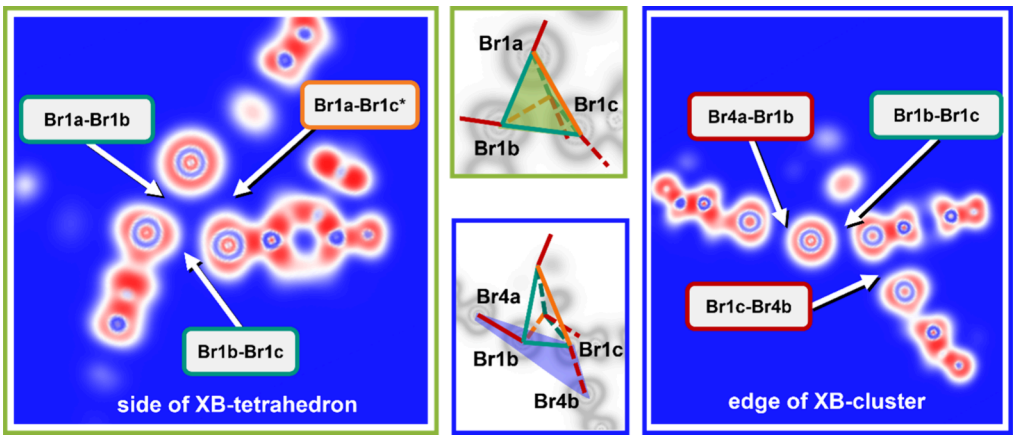

Figure 6. Analysis of the halogen bonding in the central motif by Electron Localization Function (ELF). Obtained after optimization of hydrogen positions with M06−2x/d4 DFT and def2-TZVP basis. The ELF ranges from blue (nonlocalized) to red (fully localized) with white being the intermediate. The left picture (green) shows one side of the inner distorted tetrahedron. One cannot see the σ-hole of Br1a, as the Br−C bond is roughly orthogonal to the plane. The red belt around the atom is therefore corresponding to p-electrons of this respective atom. Br1a acts as the XB_A for Br1b, which in turn acts as the XB_A for Br1c. The Br1a−Br1c* interaction on the right-hand side of the picture is not a donor−acceptor interaction because the lone pairs point toward each other. On the right-hand side (blue), a plane through the edge of the motif is shown. One can see that the inner (Br1b, Br1c) atoms are acting as the halogen bond acceptors for the outer (Br4a, Br4b) atoms. Additionally, Br1b is acting as the XB_A for Br1c, as already seen in the left picture.

Scheme 4. Models Used to Calculate the Total Interaction Energy for the XB Interactions[a]

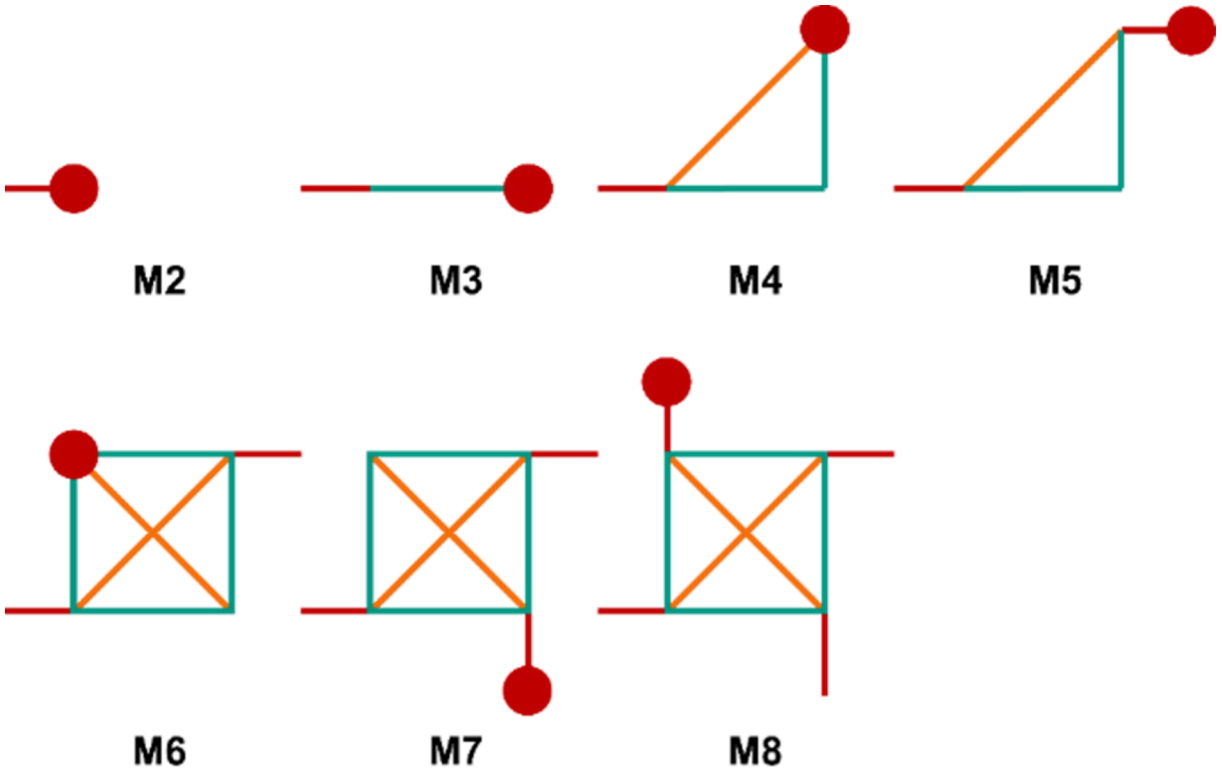

[a]Each vertex represents a *p*-bromo-*o*-vanillin. Red circles show the addition of molecules to the model. Red lines denote a Br1−Br4 interaction, green lines Br1−Br1 and orange lines Br1−Br1* interactions.

with the intermolecular distance, unsurprisingly resulting in the lowest value for the long Br1−Br1* contact. For Br3−Br5 the low exchange repulsion value is the result of an almost perfect alignment (close to 180° and 90°) of the two interacting partners with 175.6(4)° and 92.5(3)° leading to a minimization of lone pair repulsion.[33] The small amount of Pauli repulsion in the Br3−Br5 interaction has a less destabilizing effect. Therefore, the negative overall pair interaction energy makes it the strongest of the interactions investigated here.

Another important factor here is the orbital relaxation, through which Br1−Br1* gains less stabilization than the other contacts. Since there is less orbital overlap for longer distances and unfavorable angles, this interaction is dominated by dispersion which operates over longer distances. Thus, we are able to confirm the trend of the interaction energy, with shorter

contacts being dominated by electrostatics and orbital interaction whereas longer contacts are dominated by electrostatics and dispersion.[85]

These effects can be further supported by an Electron Localization Function (ELF) which quantifies the local kinetic energy excess due to Pauli repulsion and takes values between 0 and 1. For a value of 1, the probability of finding another electron of the same spin at the same position as a reference electron is 0, which means perfect localization. The ELF is formulated such that the value of 0.5 corresponds to the localization in the free electron gas.[86] Figure 6 shows two planes through the central XB-interactions involving four Br atoms of four Er_6 clusters. It is clear that while the interactions of Br1−Br1 and Br1−Br4 are XB-donor−acceptor interactions this is not the case for Br1−Br1*. The corresponding ELF plots are shown in Figure 6 and the molecular electrostatic potentials in Figures S8−S10. These demonstrate the presence of σ-holes. Furthermore, from these results it becomes apparent that all but the Br1−Br1* interaction can be classified as donor−acceptor interactions with Br1 acting as the XB-acceptor for both Br1 and Br4, Br2 as the XB-acceptor for Br6 and Br3 as the XB-acceptor for Br3, respectively.

COOPERATIVE EFFECTS IN THE CENTRAL HALOGEN BOND MOTIF OF 2

In order to explore the possibility of cooperative/synergetic effects, i.e., how multiple halogen bonds interact with each other, a stepwise formation of the cluster was calculated as illustrated in Scheme 4. In each of the seven models (M2−M8), 5-bromo-*o*-vanillin units were added as indicated by the red dot until the full cluster is constructed. For each individual step the interaction energy between the additional molecule and the previous model was calculated. Starting from a single 5-bromo-*o*-vanillin molecule, a second was added to it and their interaction energy E_{M_2} was calculated analogous to the previously described pair interactions (M2). In the next step a third molecule was added and the interaction energy between the two 5-bromo-*o*-vanillin molecules that make up M2 and the third was calculated giving model 3 (M3). The first step does not include any cooperative effects since it is simply a pair-interaction. In the second step, constructing M3, the interaction of the first XB with the second XB is included as well as the pair interaction to the newly added molecule making it possible to discern whether the overall interaction energy is higher than the simple sum over the pair interactions. This is repeated until the full cluster is constructed. Importantly, such a setup avoids double counting of interactions.

The synergy energy can thus be calculated as

$$E_{syn} = \sum_{i=2}^{i=8} E_{M_i} - (4 \cdot E_{Br1-Br1} + 4 \cdot E_{Br1-Br4} + 2 \cdot E_{Br1-Br1^*})$$

with E_{Mi} being the interaction energies obtained for each of the 7 steps.

In the ideal case it should not be necessary to do the Br for H-substitution outlined in the methodology section in order to remove those interactions between the molecules which are not related to the halogen bonding. This is discussed in more detail in the SI. Using the different functionals an average synergy contribution of −26.4 kJ/mol was calculated which is 29.4% of the total interaction energy. Similar calculations on *N*-halo-guanine- and haloamine-quartets yield comparable synergy effects with 30.3 and 18.7% for their respective Br-substituted molecules.[60,67] However, the present investigation is the first to find and quantify such synergy effects between inorganic coordination clusters.

CONCLUSIONS

In summary, we report the structures of two isostructural trigonal prismatic Er_6 clusters in which the carbonate bridges are formed via the absorption of atmospheric CO_2. These differ by a bromine atom on the Schiff base ligand. These bromine atoms allow us to generate supramolecular interactions in the form of multiple halogen−halogen bonds. Each individual Er_6 cluster makes eight halogen bonds forming a unique and unexpectedly seven-connected tetragonal network. Since this compound crystallizes in the tetragonal space group $P\bar{4}2_1c$, either six- or eight-connected network would usually be expected. The XB motif involving 8 Er_6-clusters in S_4-symmetry is, to the best of our knowledge unprecedented.

The halogen−halogen interactions in this network have been analyzed in detail using DFT, EDA, AIM and ELF calculations. The DFT calculations yielded interaction energies between 4 and 7 kJ/mol for the different Br−Br pair interactions. The EDA of all interactions was able to confirm the trend of halogen−halogen interactions in short contacts being predominantly electrostatic in nature whereas for longer contacts dispersion interaction are the dominant factor.

Although each individual halogen bond is rather weak, the whole crystal structure is significantly stabilized through cooperative effects between the halogen bonds. This means that the overall stabilization gained from the halogen bonds is greater than the sum of their individual energies. We note that such cooperative effects have rarely been investigated and, to the best of our knowledge, this is the first time such synergy has been shown for a crystallographically characterized inorganic coordination cluster compound.

The Er^{III}_6 clusters presented here provide a proof-of-principle that synergistic cooperativity between halogen bonds can significantly increase the strength of intermolecular interactions between inorganic coordination clusters creating a novel 3D network. This approach can subsequently be applied to more magnetically interesting ions such as Dy^{III}[87] to assess whether it is possible to influence the dynamic magnetic behavior of SMMs in regard to controlling spin-phonon coupling, through the strength and thus rigidity of the 3D network in order to influence phonon modes.

AUTHOR INFORMATION

Corresponding Authors

Jonas Braun − *Institute of Inorganic Chemistry, Karlsruhe Institute of Technology (KIT), 76131 Karlsruhe, Germany;*

Institute for Nanotechnology and Institute for Quantum Materials and Technologies, Karlsruhe Institute of Technology (KIT), 76131 Karlsruhe, Germany; orcid.org/0000-0002-2590-4546; Email: jonas.braun2@kit.edu

Karin Fink − *Institute for Nanotechnology, Karlsruhe Institute of Technology (KIT), 76131 Karlsruhe, Germany;* Email: karin.fink@kit.edu

Annie K. Powell − *Institute of Inorganic Chemistry, Karlsruhe Institute of Technology (KIT), 76131 Karlsruhe, Germany; Institute for Nanotechnology and Institute for Quantum Materials and Technologies, Karlsruhe Institute of Technology (KIT), 76131 Karlsruhe, Germany;* orcid.org/0000-0003-3944-7427; Email: annie.powell@kit.edu

Authors

Christian Pachl − *Institute of Inorganic Chemistry, Karlsruhe Institute of Technology (KIT), 76131 Karlsruhe, Germany; Institute for Nanotechnology, Karlsruhe Institute of Technology (KIT), 76131 Karlsruhe, Germany;* orcid.org/0009-0005-8105-0409

Olaf Fuhr − *Institute for Nanotechnology and Karlsruhe Nano Micro Facility (KNMFi), Karlsruhe Institute of Technology (KIT), 76131 Karlsruhe, Germany;* orcid.org/0000-0003-3516-2440

George E. Kostakis − *Department of Chemistry, School of Life Sciences, University of Sussex, Brighton BN1 9QJ, U.K.;* orcid.org/0000-0002-4316-4369

Jinkui Tang − *State Key Laboratory of Rare Earth Resource Utilization, Changchun Institute of Applied Chemistry, Chinese Academy of Sciences, Changchun 130022, P.R. China;* orcid.org/0000-0002-8600-7718

Christopher E. Anson − *Institute of Inorganic Chemistry, Karlsruhe Institute of Technology (KIT), 76131 Karlsruhe, Germany;* orcid.org/0000-0001-7992-7797

Author Contributions

J.B. synthetic work and characterization; J.B., C.P., C.E.A., K.F. and A.K.P. paper conceptualization, writing of original draft and editing; O.F. acquisition of single-crystal X-ray data; C.E.A. crystallography; J.T. magnetic investigation; G.E.K. topological analysis; C.P. and K.F. theoretical calculations; K.F. and A.K.P. project supervision and funding acquisition. The manuscript was written through contributions of all authors. All authors have given approval to the final version of the manuscript.

Notes

The authors declare no competing financial interest.

ACKNOWLEDGMENTS

The authors acknowledge funding by the German Research Council (DFG) through the CRC 1573 "4f for Future" and the Helmholtz POF MSE. J.B. and C.P. thank the Karlsruhe House of Young Scientists for funding through the Landesgraduierten-foerderung Baden-Wurttemberg.

REFERENCES

(1) Lehn, J.-M. Supramolecular Chemistry: Receptors, Catalysts, and Carriers. *Science* **1985**, *227*, 849−856.
(2) Steed, J. W.; Atwood, J. L. *Supramolecular Chemistry*; John Wiley & Sons, 2009.
(3) Stupp, S. I.; Palmer, L. C. Supramolecular Chemistry and Self-Assembly in Organic Materials Design. *Chem. Mater.* **2014**, *26*, 507−518.
(4) Biedermann, F.; Schneider, H. J. Experimental Binding Energies in Supramolecular Complexes. *Chem. Rev.* **2016**, *116*, 5216−5300.
(5) Aakeröy, C. B. Crystal Engineering: Strategies and Architectures. *Acta Cryst. B* **1997**, *53*, 569−586.
(6) Braga, D.; Brammer, L.; Champness, N. R. New trends in crystal engineering. *CrystEngComm* **2005**, *7*, 1−19.
(7) Braga, D.; Grepioni, F.; Desiraju, G. R. Crystal Engineering and Organometallic Architecture. *Chem. Rev.* **1998**, *98*, 1375−1405.
(8) Claessens, C. G.; Stoddart, J. F. Pi-Pi Interactions in Self-Assembly. *J. Phys. Org. Chem.* **1997**, *10*, 254−272.
(9) MacDonald, J. C.; Dorrestein, P. C.; Pilley, M. M.; Foote, M. M.; Lundburg, J. L.; Henning, R. W.; Schultz, A. J.; Manson, J. L. Design of Layered Crystalline Materials Using Coordination Chemistry and Hydrogen Bonds. *J. Am. Chem. Soc.* **2000**, *122*, 11692−11702.
(10) Jeffrey, G. A. *An Introduction to Hydrogen Bonding*; Oxford University Press, 1997.
(11) Pauling, L. *The nature of the chemical bond and the structure of molecules and crystals: An Introduction to Modern Structural Chemistry*; Cornell University Press, 1960.
(12) Grimme, S. Do special noncovalent pi-pi stacking interactions really exist? *Angew. Chem., Int. Ed.* **2008**, *47*, 3430−3434.
(13) Hunter, C. A.; Lawson, K. R.; Perkins, J.; Urch, C. J. Aromatic interactions. *J. Chem. Soc., Perkin Trans. 2* **2001**, 651−669.
(14) Hunter, C. A.; Sanders, J. K. M. The Nature of Pi-Pi Interactions. *J. Am. Chem. Soc.* **1990**, *112*, 5525−5534.
(15) Ma, J. C.; Dougherty, D. A. The Cation−π Interaction. *Chem. Rev.* **1997**, *97*, 1303−1324.
(16) Martinez, C. R.; Iverson, B. L. Rethinking the term "pi-stacking". *Chem. Sci.* **2012**, *3*, 2191−2201.
(17) Rather, I. A.; Wagay, S. A.; Ali, R. Emergence of anion-π interactions: The land of opportunity in supramolecular chemistry and beyond. *Coord. Chem. Rev.* **2020**, *415*, No. 213327.
(18) Dzyaloshinskii, I. E.; Lifshitz, E. M.; Pitaevskii, L. P. The general theory of van der Waals forces. *Adv. Phys.* **1961**, *10*, 165−209.
(19) Israelachvili, J. N. The nature of van der waals forces. *Contemp. Phys.* **1974**, *15*, 159−177.
(20) London, F. Über das Verhältnis der van der Waalsschen Kräfte zu den homöopolaren Bindungskräften. *Z. Phys.* **1930**, *60*, 491−527.
(21) Winterton, R. H. S. Van der Waals forces. *Contemp. Phys.* **1970**, *11*, 559−574.
(22) Huang, B.; Clark, G.; Navarro-Moratalla, E.; Klein, D. R.; Cheng, R.; Seyler, K. L.; Zhong, D.; Schmidgall, E.; McGuire, M. A.; Cobden, D. H.; et al. Layer-dependent ferromagnetism in a van der Waals crystal down to the monolayer limit. *Nature* **2017**, *546*, 270−273.
(23) Shah, S.; Marandi, P.; Neelakandan, P. P. Advances in the Supramolecular Chemistry of Tetracoordinate Boron-Containing Organic Molecules into Organogels and Mesogens. *Front. Chem.* **2021**, *9*, No. 708854.
(24) Watson, J. D.; Crick, F. H. C. Molecular Structure of Nucleic Acids. *Nature* **1953**, *171*, 737−738.
(25) Zhao, Y.; Truhlar, D. G. Multicoefficient Extrapolated Density Functional Theory Studies of $\pi_{,,,}\pi$ Interactions: The Benzene Dimer. *J. Phys. Chem. A Lett.* **2005**, *109*, 4209−4212.
(26) Cavallo, G.; Metrangolo, P.; Milani, R.; Pilati, T.; Priimagi, A.; Resnati, G.; Terraneo, G. The Halogen Bond. *Chem. Rev.* **2016**, *116*, 2478−2601.
(27) Hassel, O. Structural Aspects of Interatomic Charge-Transfer Bonding. *Science* **1970**, *170*, 497−502.
(28) Hassel, O.; Hvoslef, J. The Structure of Bromine 1,4-Dioxanate. *Acta Chem. Scand.* **1954**, *8*, 873−873.
(29) Clark, T.; Hennemann, M.; Murray, J. S.; Politzer, P. Halogen bonding: the sigma-hole. *J. Mol. Model.* **2007**, *13*, 291−296.
(30) Metrangolo, P.; Neukirch, H.; Pilati, T.; Resnati, G. Halogen Bonding Based Recognition Processes: A World Parallel to Hydrogen Bonding. *Acc. Chem. Res.* **2005**, *38*, 386−395.

(31) Politzer, P.; Lane, P.; Concha, M. C.; Ma, Y.; Murray, J. S. An overview of halogen bonding. *J. Mol. Model* **2007**, *13*, 305−311.
(32) Metrangolo, P.; Meyer, F.; Pilati, T.; Resnati, G.; Terraneo, G. Halogen bonding in supramolecular chemistry. *Angew. Chem. Int. Ed.* **2008**, *47*, 6114−6127.
(33) Huber, S. M.; Scanlon, J. D.; Jimenez-Izal, E.; Ugalde, J. M.; Infante, I. On the directionality of halogen bonding. *Phys. Chem. Chem. Phys.* **2013**, *15*, 10350−10357.
(34) Priimagi, A.; Cavallo, G.; Metrangolo, P.; Resnati, G. The Halogen Bond in the Design of Functional Supramolecular Materials: Recent Advances. *Acc. Chem. Res.* **2013**, *46*, 2686−2695.
(35) Mukherjee, A.; Tothadi, S.; Desiraju, G. R. Halogen bonds in crystal engineering: like hydrogen bonds yet different. *Acc. Chem. Res.* **2014**, *47*, 2514−2524.
(36) Carter, K. P.; Zulato, C. H. F.; Cahill, C. L. Exploring supramolecular assembly and luminescent behavior in a series of RE-p-chlorobenzoic acid-1,10-phenanthroline complexes. *CrystEngComm* **2014**, *16*, 10189−10202.
(37) Fukuroi, K.; Takahashi, K.; Mochida, T.; Sakurai, T.; Ohta, H.; Yamamoto, T.; Einaga, Y.; Mori, H. Synergistic spin transition between spin crossover and spin-Peierls-like singlet formation in the halogen-bonded molecular hybrid system: $[Fe(Iqsal)_2][Ni(dmit)_2]\cdot CH_3CN\cdot H_2O$. *Angew. Chem. Int. Ed.* **2014**, *53*, 1983−1986.
(38) Carter, K. P.; Thomas, K. E.; Pope, S. J.; Holmberg, R. J.; Butcher, R. J.; Murugesu, M.; Cahill, C. L. Supramolecular Assembly of Molecular Rare-Earth-3,5-Dichlorobenzoic Acid-2,2':6',2''-Terpyridine Materials: Structural Systematics, Luminescence Properties, and Magnetic Behavior. *Inorg. Chem.* **2016**, *55*, 6902−6915.
(39) Carter, K. P.; Pope, S. J. A.; Kalaj, M.; Holmberg, R. J.; Murugesu, M.; Cahill, C. L. Exploring the Promotion of Synthons of Choice: Halogen Bonding in Molecular Lanthanide Complexes Characterized via X-ray Diffraction, Luminescence Spectroscopy, and Magnetic Measurements. *Z. Anorg. Allg. Chem.* **2017**, *643*, 1948−1955.
(40) Lazaro, S. E.; Alkas, A.; Lee, S. J.; Telfer, S. G.; Murray, K. S.; Phonsri, W.; Harding, P.; Harding, D. J. Abrupt spin crossover in iron(III) complexes with aromatic anions. *Dalton Trans.* **2019**, *48*, 15515−15520.
(41) Atzori, M.; Artizzu, F.; Sessini, E.; Marchio, L.; Loche, D.; Serpe, A.; Deplano, P.; Concas, G.; Pop, F.; Avarvari, N.; et al. Halogen-bonding in a new family of tris(haloanilato)metallate(III) magnetic molecular building blocks. *Dalton Trans.* **2014**, *43*, 7006−7019.
(42) Busch, R.; Carter, A. B.; Konidaris, K. F.; Kuhne, I. A.; Gonzalez, R.; Anson, C. E.; Powell, A. The first use of a ReX5 synthon to modulate FeIII spin crossover via supramolecular halogenhalogen interactions. *Chem. Eur. J.* **2020**, *26*, 11835−11840.
(43) Jiang, Y.; Hayes, S.; Bittmann, S.; Sarracini, A.; Liu, L. C.; Muller-Werkmeister, H. M.; Miyawaki, A.; Hada, M.; Nakano, S.; Takahashi, R.; et al. Direct observation of photoinduced sequential spin transition in a halogen-bonded hybrid system by complementary ultrafast optical and electron probes. *Nat. Commun.* **2024**, *15*, 4604.
(44) Mulliken, R. S. P. Structures of Complexes Formed by Halogen Molecules with Aromatic and with Oxygenated Solvents. *J. Am. Chem. Soc.* **1950**, *72*, 600−608.
(45) Flurry, R. L., Jr Molecular Orbital Theory of Electron Donor-Acceptor Complexes. I. A Simple Semiempirical Treatment. *J. Phys. Chem.* **1965**, *69*, 1927−1933.
(46) Bent, H. A. Structural Chemistry of Donor-Acceptor Interactions. *Chem. Rev.* **1968**, *68*, 587−648.
(47) Flurry, R. L., Jr Molecular Orbital Theory of Electron Donor-Acceptor Complexes. II. Charged Donors and Acceptors. *J. Phys. Chem.* **1969**, *75*, 2111−2117.
(48) Brinck, T.; Murray, J. S.; Politzer, P. Surface Electrostatic Potentials of Halogenated Methanes as Indicators of Directional Intermolecular Interactions. *Int. J. Quantum Chem.* **1992**, *44*, 57−64.
(49) Lu, Y.-X.; Zou, J.-W.; Wang, Y.-H.; Jiang, Y.-J.; Yu, Q.-S. Ab Initio Investigation of the Complexes between Bromobenzene and Several Electron Donors: Some Insights into the Magnitude and Nature of Halogen Bonding Interactions. *J. Phys. Chem. A* **2007**, *111*, 10781−10788.
(50) Riley, K. E.; Murray, J. S.; Politzer, P.; Concha, M. C.; Hobza, P. Br ···O Complexes as Probes of Factors Affecting Halogen Bonding: Interactions of Bromobenzenes and Bromopyrimidines with Acetone. *J. Chem. Theory Comput.* **2009**, *5*, 155−163.
(51) Wallnoefer, H. G.; Fox, T.; Liedl, K. R.; Tautermann, C. S. Dispersion dominated halogen-pi interactions: energies and locations of minima. *Phys. Chem. Chem. Phys.* **2010**, *12*, 14941−14949.
(52) Anderson, L. N.; Aquino, F. W.; Raeber, A. E.; Chen, X.; Wong, B. M. Halogen Bonding Interactions: Revised Benchmarks and a New Assessment of Exchange vs Dispersion. *J. Chem. Theory Comput.* **2018**, *14*, 180−190.
(53) Boys, S. F.; Bernardi, F. The calculation of small molecular interactions by the differences of separate total energies. Some procedures with reduced errors. *Mol. Phys.* **1970**, *19*, 553−566.
(54) Alvarez-Idaboy, J. R.; Galano, A. Counterpoise corrected interaction energies are not systematically better than uncorrected ones: comparison with CCSD(T) CBS extrapolated values. *Theor. Chem. Acc.* **2010**, *126*, 75−85.
(55) Li, D.; Xia, T.; Feng, W.; Cheng, L. Revisiting the covalent nature of halogen bonding: a polarized three-center four-electron bond. *RSC Adv.* **2021**, *11*, 32852−32860.
(56) Xantheas, S. S. Ab initio studies of cyclic water clusters $(H_2O)_n$, n = 1−6. II. Analysis of many-body interactions. *J. Chem. Phys.* **1994**, *100*, 7523−7534.
(57) Xantheas, S. S. Cooperativity and hydrogen bonding network in water clusters. *Chem. Phys.* **2000**, *258*, 225−231.
(58) Dominikowska, J. Halogen-bonded haloamine trimers - modelling the X_3 synthon. *Phys. Chem. Chem. Phys.* **2020**, *22*, 21938−21946.
(59) Dominikowska, J.; Rybarczyk-Pirek, A. J.; Fonseca Guerra, C. Lack of Cooperativity in the Triangular X3 Halogen-Bonded Synthon? *Cryst. Growth Des.* **2021**, *21*, 597−607.
(60) Dominikowska, J.; Bickelhaupt, F. M.; Palusiak, M.; Fonseca Guerra, C. Source of Cooperativity in Halogen-Bonded Haloamine Tetramers. *ChemPhysChem* **2016**, *17*, 474−480.
(61) Parra, R. D. Cooperative effects and energy barriers to bromonium ion transfer in cyclic (BrX)n halogen-bonded clusters (X = F, OH, or NH2; n = 3−5): An ab initio study. *Comput. Theor. Chem.* **2015**, *1066*, 47−54.
(62) Parra, R. D. Cooperative strengthening of the halogen bond in cyclic clusters of iodine monofluoride, (IF)n (n = 3−8): From a closed-shell interaction, F-I···F, to a symmetric partly covalent interaction, F···I···F. *Chem. Phys. Lett.* **2022**, *803*, No. 139825.
(63) Scheiner, S. Properties and Stabilities of Cyclic and Open Chains of Halogen Bonds. *J. Phys. Chem. A* **2022**, *126*, 6443−6455.
(64) George, J.; Deringer, V. L.; Dronskowski, R. Cooperativity of halogen, chalcogen, and pnictogen bonds in infinite molecular chains by electronic structure theory. *J. Phys. Chem. A* **2014**, *118*, 3193−3200.
(65) Vermeeren, P.; Wolters, L. P.; Paragi, G.; Fonseca Guerra, C. Cooperative Self-Assembly in Linear Chains Based on Halogen Bonds. *ChemPlusChem.* **2021**, *86*, 812−819.
(66) Masoodi, H. R.; Bagheri, S.; Ranjbar, M. Theoretical study of cooperativity between hydrogen bond-hydrogen bond, halogen bond-halogen bond and hydrogen bond-halogen bond in ternary FX··· diazine···XF (X = H and Cl) complexes. *Mol. Phys.* **2016**, *114*, 3464−3474.
(67) Wolters, L. P.; Smits, N. W.; Guerra, C. F. Covalency in resonance-assisted halogen bonds demonstrated with cooperativity in N-halo-guanine quartets. *Phys. Chem. Chem. Phys.* **2015**, *17*, 1585−1592.
(68) Tian, H.; Wang, M.; Zhao, L.; Guo, Y. N.; Guo, Y.; Tang, J.; Liu, Z. A discrete dysprosium trigonal prism showing single-molecule magnet behaviour. *Chem. Eur. J.* **2012**, *18*, 442−445.
(69) Tian, H.; Zhao, L.; Guo, Y. N.; Guo, Y.; Tang, J.; Liu, Z. Quadruple-CO32- bridged octanuclear dysprosium(III) compound showing single-molecule magnet behaviour. *Chem. Commun.* **2012**, *48*, 708−710.

(70) Tian, H.; Zhao, L.; Lin, H.; Tang, J.; Li, G. Butterfly-shaped pentanuclear dysprosium single-molecule magnets. *Chem. – Eur. J.* **2013**, *19*, 13235–13241.
(71) Tian, H.; Ungur, L.; Zhao, L.; Ding, S.; Tang, J.; Chibotaru, L. F. Exchange Interactions Switch Tunneling: A Comparative Experimental and Theoretical Study on Relaxation Dynamics by Targeted Metal Ion Replacement. *Chem. – Eur. J.* **2018**, *24*, 9928–9939.
(72) Braun, J.; Seufert, D.; Anson, C. E.; Tang, J.; Powell, A. K. An Effectively Uncoupled Gd8 Cluster Formed through Fixation of Atmospheric CO2 Showing Excellent Magnetocaloric Properties. *Int. J. Mol. Sci.* **2024**, *25*, 264.
(73) Pineda, E. M.; Lorusso, G.; Zangana, K. H.; Palacios, E.; Schnack, J.; Evangelisti, M.; Winpenny, R. E. P.; McInnes, E. J. L. Observation of the influence of dipolar and spin frustration effects on the magnetocaloric properties of a trigonal prismatic Gd7 molecular nanomagnet. *Chem. Sci.* **2016**, *7*, 4891–4895.
(74) Goura, J.; Colacio, E.; Herrera, J. M.; Suturina, E. A.; Kuprov, I.; Lan, Y.; Wernsdorfer, W.; Chandrasekhar, V. Heterometallic Zn(3) Ln(3) Ensembles Containing (mu(6) -CO(3)) Ligand and Triangular Disposition of Ln(3+) ions: Analysis of Single-Molecule Toroic (SMT) and Single-Molecule Magnet (SMM) Behavior. *Chem. Eur. J.* **2017**, *23*, 16621–16636.
(75) Maity, S.; Ghosh, T. K.; Ito, S.; Bhunia, P.; Ishida, T.; Ghosh, A. Structures and Magnetic Properties of Carbonato-Bridged Hexanuclear NiII4LnIII2 (Ln = Gd, Tb, Dy) Complexes Formed by Atmospheric Carbon Dioxide Fixation in the Absence of an External Base. *Cryst. Growth Des.* **2022**, *22*, 4332–4342.
(76) Kanazawa, Y.; Kamitani, M. Rare earth minerals and resources in the world. *J. Alloys Compd.* **2006**, *408–412*, 1339–1343.
(77) Bondi, A. van der Waals Volumes and Radii. *J. Phys. Chem.* **1964**, *68*, 441–451.
(78) Blatov, V. A.; Shevchenko, A. P.; Proserpio, D. M. Applied Topological Analysis of Crystal Structures with the Program Package ToposPro. *Cryst. Growth Des.* **2014**, *14*, 3576–3586.
(79) Solimannejad, M.; Malekani, M.; Alkorta, I. Substituent effects on the cooperativity of halogen bonding. *J. Phys. Chem. A* **2013**, *117*, 5551–5557.
(80) Caldeweyher, E.; Bannwarth, C.; Grimme, S. Extension of the D3 dispersion coefficient model. *J. Chem. Phys.* **2017**, *147*, No. 034112.
(81) Caldeweyher, E.; Ehlert, S.; Hansen, A.; Neugebauer, H.; Spicher, S.; Bannwarth, C.; Grimme, S. A generally applicable atomic-charge dependent London dispersion correction. *J. Chem. Phys.* **2019**, *150*, 154122.
(82) Kozuch, S.; Martin, J. M. Halogen Bonds: Benchmarks and Theoretical Analysis. *J. Chem. Theory Comput.* **2013**, *9*, 1918–1931.
(83) Siiskonen, A.; Priimagi, A. Benchmarking DFT methods with small basis sets for the calculation of halogen-bond strengths. *J. Mol. Model* **2017**, *23*, 50.
(84) Riley, K. E.; Hobza, P. The relative roles of electrostatics and dispersion in the stabilization of halogen bonds. *Phys. Chem. Chem. Phys.* **2013**, *15*, 17742–17751.
(85) Kolár, M. H.; Deepa, P.; Ajani, H.; Pecina, A.; Hobza, P. Characteristics of a σ-Hole and the Nature of a Halogen Bond. In *Halogen Bonding II. Topics in Current Chemistry*; Metrangolo, P.; Resnati, G., Eds.; vol 359; Springer, 2015; pp 1–25.
(86) Becke, A. D.; Edgecombe, K. E. A simple measure of electron localization in atomic and molecular systems. *J. Chem. Phys.* **1990**, *92*, 5397–5403.
(87) Langley, S. K.; Vignesh, K. R.; Moubaraki, B.; Rajaraman, G.; Murray, K. S. Oblate versus Prolate Electron Density of Lanthanide Ions: A Design Criterion for Engineering Toroidal Moments? A Case Study on $\{Ln^{III}_6\}$ (Ln = Tb, Dy, Ho and Er) Wheels. *Chem. – Eur. J.* **2019**, *25*, 4156–4165.